SI Appendix

Computational Details

We built the method of Pophale *et al*. to carry out the computations, here considering chirality of the OSDA (1). The DREIDING forcefield was used in the GULP simulation program to carry out the calculations. The OSDA identified in Schmidt *et al.* was found to occupy the cages of STW at a loading of two per cage (2). We carried out a combinatorial search of two OSDA monomers, linked by the Menshutkin reaction to a halogenated carbon chain. We obtained the linkers from the shelf and also extended the shelf by applying all zero-order reactions and brominating the resulting compounds having a OH group. We required the constructed molecules to contain two chiral centers, no more than 8 torsions, and between 2 and 4 quaternary amines. In all, we considered 644 linked diquats. The stabilization energies of all chiral enantiomorphs were calculated, and the energy gap between the most and second most stable form was computed. The stabilization energy was computed as in Pophale *et al*., *via* geometric placement of the OSDAs in the zeolite, four energy minimizations, followed by three increasingly longer molecular dynamics runs at 343 K (1).

Experimental Methods

1. Sources of chemicals

trans-2-Phenylcyclopropane-1-carboxylic acid (Sigma-Aldrich, 95%), quinine (Sigma-Aldrich, anhydrous, ≥98%), +-dehydroabietylamine (Sigma-Aldrich, 60%), toluene (EMD Millipore, ≥99.5%), glacial acetic acid (EMD Millipore, 99%), hexane (EMD Millipore, ≥95%), water (house still, ≥99.99%), sodium hydroxide (Alfa Aesar, 97%), diethyl ether (EMD Millipore, ≥99.0%), potassium carbonate (Sigma-Aldrich, anhydrous, 99.99% trace metals basis), methanol (EMD Millipore, ≥99.8%), sodium bicarbonate (Sigma-Aldrich, ≥99.7%),

hydrochloric acid (Sigma-Aldrich, 37%), magnesium sulfate (Sigma-Aldrich, anhydrous, ≥99.5%), chloroform (EMD Millipore, ≥99.8%), ethyl acetate (EMD Millipore, ≥99.5%), hydrogen peroxide (EMD Millipore, 30% (w/w) in water), tetrahydrofuran (EMD Millipore, ≥99.5%), lithium aluminum hydride (Sigma-Aldrich, 95%), ammonium chloride (Sigma-Aldrich, ≥99.7%), bromine (Sigma-Aldrich, ≥99.5%), triphenylphosphine (Sigma-Aldrich, 99%), acetonitrile (Sigma-Aldrich, anhydrous, 99.8%), tetramethylimidazole (TCI Chemicals, ≥98%), Dowex Marathon A, hydroxide from (Sigma-Alrich), [Tetrabutylammonium] [(Λ,R)-(1,1′-binaphthalene-2,2′diolato) (bis (tetrachlor-1,2-benzenediolato) phosphat(V))] (Sigma-Aldrich, ≥95%), tetraethylorthosilicate (Sigma-Aldrich, 98%), hydrofluoric acid (Sigma-Aldrich, 48% (w/w) in water), aluminum isopropoxide (Sigma-Aldrich, ≥99.99% trace metals basis), germanium oxide (Strem, 99.99%) were purchased and used as received.

2. Synthesis and NMR Characterization of the Chiral Organic Structure Directing Agent

A summary of the synthesis method implemented to develop both the R- and S-enantiomers of the organic structure directing agent used in this study is detailed in Fig. S1 (chiral separation) and Fig. S2 (reaction pathway).

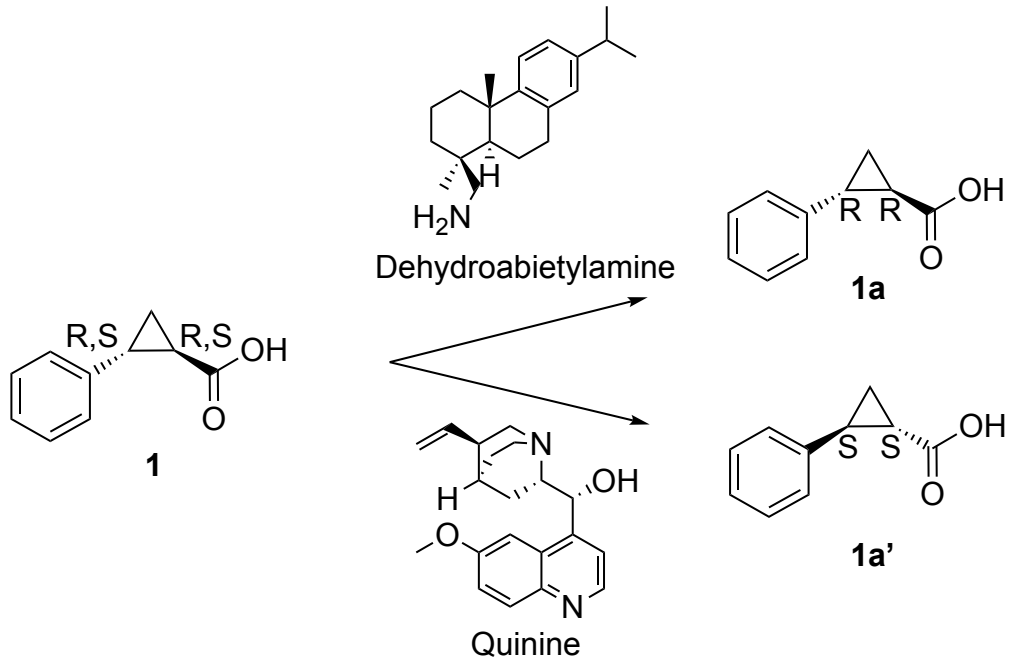

Fig. S1. Chiral resolution scheme of trans-2-phenylcyclopropane-1-carboxylic acid using dehydroabietylamine or quinine to yield **1a** or **1a'**, respectively. (3, 4)

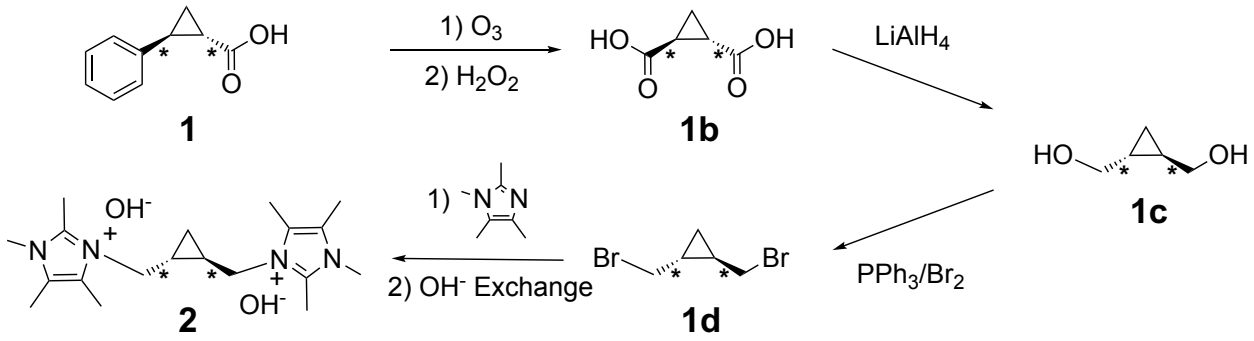

Fig. S2. Scheme for the synthesis of the racemic OSDA **2** from **1**. Note that the same synthesis procedure can be applied to **1a** or **1a'** to yield R-**2** or S-**2**, respectively.

Separation of the Enantiomers of **1**

Several methods have been described to separate what are denoted the (-)-R (**1a**) and (+)-S (**1a'**) enantiomers of trans-2-phenylcyclopropanecarboxylic acid (**1**) using either quinine and brucine or dehydroabietylamine, respectively (3, 4). In this work, brucine was avoided due to the toxicity of this compound.

Chiral Resolution of (1R,2R)-2-Phenylcyclopropane-1-carboxylic acid (**1a**)

The purification of dehydroabietylamine was conducted by the method reported by Gottstein (5). 900 g of dehydroabietylamine was dissolved in 1.5 liters of toluene. Then a solution of 210 g of glacial acetic acid in 500 mL of toluene was added. The solution was then refrigerated overnight and the product was collected *via* filtration and washed with cold toluene. The product was recrystallized one time from toluene and washed with hexane and dried under vacuum to yield 490 g of purified dehydroabietylamine acetate.

Dehydroabietylamine acetate (490 g) was dissolved in 630 mL of boiling water. Then 500 mL of 10% NaOH solution were added. After the mixture was chilled it was extracted several times with diethyl ether, the combined extracts were washed with water and dried over anhydrous potassium carbonate. The ether was then removed using rotary evaporation to yield 357 g of a yellow oil that slowly solidified.

The enantiopurification was performed according to the method of Cheng *et al*. (4). 150 g of **1** (racemic mixture from Aldrich, MW=162.19, 925 mmol) was dissolved in 940 mL of warm methanol. Then 263 g of purified dehydroabietylamine (925 mmol) was dissolved separately in 750 mL of warm methanol. The two solutions were slowly combined (Caution: Exothermic process, use caution) and, after sitting at room temperature overnight, the resultant solid salt of dehydroabietylamine and **1a** was recovered using filtration and was then recrystallized from 90% aqueous methanol six times to yield a solid with a rotation of $[\alpha]_D^{20}$ −81° (*c* 0.42, MeOH) (literature: $[\alpha]_D^{20}$ −80.8° (*c* 0.61, MeOH)) (4). The total mass of recovered solids was 78.5 g.

The free acid was isolated by adding the salt dehydroabietylamine and **1a** to a saturated solution of $NaHCO_3$ and then extracting with diethyl ether. The aqueous fraction was then acidified with 37% hydrochloric acid followed by successive extractions with diethyl ether. The

organic extractions were combined, dried over anhydrous magnesium sulfate and then the solvent removed using rotary evaporation to yield 18.1 g of enantiopure **1a**. The rotation of **1a** in chloroform was found to be $[\alpha]_D^{20}$ -375.6° (*c* 1.07, $CHCl_3$) (literature: $[\alpha]_D^{20}$ -401° (*c* 0.88, $CHCl_3$)) (4).

Chiral Resolution of (1S,2S)-2-Phenylcyclopropane-1-carboxylic acid (**1a'**)

Following the method of Cheng *et al*. and Overberger *et al*., 125 g of **1** (racemic mixture from Aldrich, MW=162.19, 771 mmol) were added to 250 g of quinine (Aldrich, MW=324.42, 771 mmol) in 4 L of ethyl acetate at reflux (3, 4). The mixture was then allowed to cool to room temperature and allowed to sit at room temperature for 1 week, over which time large white crystals of the salt of quinine and **1a**' precipitated from the solution. The crystals were recovered by filtration, and the filtrate was then recrystallized an additional 5 times from ethyl acetate to yield a white product with a rotation of $[\alpha]_D^{20}$ -10.0° (*c* 1.0, EtOH) (literature: $[\alpha]_D^{20}$ -10.2° (*c* 1.0, EtOH)] (4). The total yield of the salt at was 95.1 g.

The free-acid product was recovered by dissolving 46.6 g of the salt of quinine and **1a**' in 500 mL of 1 M HCl at room temperature. **1a'** was then recovered by extraction with diethyl ether to yield 15.0 g. The rotation of **1a'** in chloroform was found to be $[\alpha]_D^{20}$ +370.8° (*c* 1.07, $CHCl_3$) (literature: $[\alpha]_D^{20}$ +406° (*c* 1.0, $CHCl_3$)) (4).

For both **1a** and **1a'**, further crystallization steps did not alter the polarimetry experiments. Additionally, the ^1H NMR of both compounds was identical to the starting material ($CDCl_3$, 500 MHz): δ 7.0-7.2 (m, 5H, Ph), 2.52 (m, 1H), 1.83 (m, 1H), 1.59 (m, 1H), 1.33 (m, 1H).

The synthesis procedures detailed below are written from the perspective of using a racemic starting material. However, the exact same procedures can be applied for the enantiopure starting materials **1a** and **1a'** to obtain R-**2** and S-**2**, respectively.

Trans-2-phenylcyclopropane carboxylic acid (**1**) to trans-1,2-cyclopropane carboxylic acid (**1b**)

1b was prepared by ozonolysis of **1** (either enantiomer, or the racemic mixture) in acetic acid according to the procedure reported by Inouye *et al*. (6). In a typical synthesis 11.6 g of **1a** (MW=162.19) was dissolved in 200 mL of glacial acetic acid. A stream of ozone was bubbled through the mixture with stirring (125 mL/minute of 6.7% ozone in O_2) at 50°C. The mixture was allowed to react for 36 hours. The reaction was cooled, and 50 mL of 30% aqueous H_2O_2 was added and stirred overnight. All liquid was then removed using vacuum distillation. Then, an additional 50 mL of 30% aqueous H_2O_2 was added, stirred for several hours, and the liquid again removed using vacuum distillation. This was repeated a total of 4 times, and the recovered solids were dried under vacuum. A total of 7.49 g of solid **1b** was recovered (MW=130.10). ^{1}H NMR (D_2O, 500 MHz): δ 2.04 (m, 2H), 1.39 (m, 2H). ^{13}C NMR (D_2O, 500 MHz): δ 175.7, 22.1, 15.3.

Trans-1,2-cyclopropane carboxylic acid (**1b**) to Trans-1,2-cyclopropane diol (**1c**)

The procedure for the reduction of **1b** to **1c** was adapted from Taylor *et al*. (7) 200 mL of THF in a 1 L round-bottom flask (RBF) were cooled in an ice bath under a nitrogen atmosphere. Then 14.95 g of $LiAlH_4$ was slowly added and stirred for 1 hour. 25 g of **1b** (Aldrich) was dissolved in THF and the slowly added to the $LiAlH_4$ suspension using a dropping funnel. After the addition was complete the mixture was stirred at 0 °C for 2 hours. Then, the RBF was removed from the ice bath and slowly allowed to warm up to room temperature and stirred for 2 hours. Finally, the reaction was heated to reflux and stirred overnight. The mixture was then

cooled in an ice bath and 60 g of saturated ammonium chloride solution was slowly added, followed by100 mL of ethyl acetate. The suspension was stirred for 4 hours and then filtered. The retentate was resuspended in additional ethyl acetate, stirred an additional 4 hours and then filtered once again. The liquid filtrate was combined and dried over magnesium sulfate. After removing the magnesium sulfate by filtration, the solvent was removed using rotary evaporation to yield a yellow oil. The yield of **1c** was 9.54 g (93.4 mmol, 70%) and was used without further purification. ^{1}H NMR ($CDCl_3$, 500 MHz): δ 5.05 (s, 2H), 3.76 (m, 2H), 3.07 (m, 2H), 1.01 (m, 2H), 0.43 (m, 2H). ^{13}C NMR ($CDCl_3$, 500 MHz): δ 65.8, 19.8, 7.2.

Trans-1,2-cyclopropane diol (**1c**) to Trans-1,2-dibromocyclopropane (**1d**)

1d was prepared following a method reported by de la Fuente *et al*. (8). In a typical reaction, 16.04 g of bromine was added to a solution of 26.32 g triphenylphosphine in dry acetonitrile (200 mL) at 273 K. A solution of 5 g of **1c** in dry acetonitrile (100 mL) was added to the reaction mixture, which was then stirred under an argon purge overnight at room temperature. Remaining acetonitrile was subsequently evaporated to yield a clear oil as well as a white triphenylphosphine oxide solid. This crude mixture was finely dispersed in hexane (2 x 250 mL) and filtered to remove the triphenylphosphine oxide. The hexane solution was evaporated under vacuum to give 4.0 g of **1d**. If necessary, **1d** was purified using column chromatography on silica gel with hexane/ethyl ether (95:5) as the eluent. ^{1}H NMR ($CDCl_3$, 500 MHz): 3.35 (m, 4H), 1.33 (m, 2H), 0.86 (m, 2H). ^{13}C NMR ($CDCl_3$, 500 MHz): 37.0, 24.4, 17.3.

Trans-1,2-dibromocyclopropane (**1d**) to Final OSDA Product (**2**)

Compound **1d** was dissolved in chloroform and then a 10% excess of tetramethylimidazole was added and the solution was refluxed overnight. After the reaction was complete, the reaction mixture was cooled to room temperature and then the diquaternary

product was extracted using water (3 times). The water was removed using rotary evaporation and the resulting solid was then dried under vacuum overnight. Finally, the product was recrystallized from chloroform to yield a white product in quatitative yield. ^{1}H NMR ($CDCl_3$, 500 MHz): δ 4.80 (m, 1H), 4.04 (m, 1H), 3.74 (s, 3H), 2.99 (s, 3H), 2.31 (s, 3H), 2.24 (s, 3H), 1.73 (m, 1H), 0.85 (t, 2H). ^{13}C NMR ($CDCl_3$, 500 MHz): δ 143.2, 125.8, 125.1, 48.2, 32.8, 17.4, 12.4, 10.6, 9.5, 9.1.

Prior to use in inorganic syntheses, **2** was ion exchanged to hydroxide form using Dowex Marathon A exchange resin and the final product concentration was determined using a Mettler-Toledo DL22 autotitrator using 0.01 M HCl as the titrant.

Characterization of the Enantiopurity of **2**

A survey of the literature finds that the enantiodiscrimination of quaternary (and diquaternary) ammonium compounds can be challenging. One method that has seen published success for this is the chiral shift reagent, Tetrabutylammonium][(Λ,R)-(1,1′-binaphthalene-2,2′diolato)(bis(tetrachlor-1,2-benzenediolato)phosphat(V)) (BINPHAT) (9–12). In a typical NMR experiment, BINPHAT was mixed in equimolar amounts (according to charge) with **2** in boiling $CDCl_3$ and the product was studied using ^{1}H NMR.

3. Synthesis and Characterization of STW

Synthesis of germanosilicate STW using OSDA **2**

STW was synthesized by methods adopted from those previously reported (2, 13). Conditions under which germanosilicate STW was found to crystallize most successfully were found to stem from starting gel compositions of 1 SiO_2:0.5 GeO_2:4 H_2O:0.5 HF:0.5 **2** (enantiopure or racemic). For a typical reaction, the desired quantity of germanium oxide and OSDA were mixed, and the solids were allowed to homogenize over the period of an hour. Next,

a quantity of tetraethylorthosilicate was added, and the mixture was allowed to hydrolyze over the period of 12 hours. Ethanol produced as a consequence of the hydrolysis was then allowed to evaporate at room temperature, in addition to a quantity of water to attain the desired H_2O/SiO_2 ratio. After allowing the gel to age at its final composition for 24 hours, as-synthesized, racemic, pure-silica STW (particle size ~1 μm) was added as seed material (10% (w/w) of SiO_2 in the gel) to this gel and mixed. The final gel was transferred to a Teflon-lined stainless steel autoclave and heated at 433 K in a rotating oven until crystallization products formed. The recovered solids were centrifuged, washed extensively with water and acetone, then dried in an oven at 343 K. To remove the organic occluded within the structure, the sample was placed into a tube furnace maintained at 423 K through which ozone was passed (125 mL/minute of 6.7% ozone in O_2). For materials with less germanium content, the solids were calcined in flowing air (100 mL min^{-1}, Airgas, breathing grade) at 853 K (after a ramp of 1 K min^{-1}) for 6 hours after maintaining 423 K for 3 hours.

Synthesis of aluminogermanosilicate STW using OSDA **2**

Aluminogermanosilicate STW was synthesized using a similar procedure outlined *vide supra* for germanosilicate STW. However, to the initial combination of germanium oxide and OSDA, a quantity of aluminum isopropoxide was added and allowed to homogenize and hydrolyze. The final gel composition of samples used in catalytic function testing were: 1 SiO_2:0.5 GeO_2:0.01 Al_2O_3:5 H_2O:0.5 HF:0.5 **2** (enantiopure or racemic). Similar procedures were also followed to remove the organic content.

Table S1. Summary of STW syntheses using racemic **2**. A = amorphous, U = unknown, synthesis time is reported in days. [1]A mixture of **2** and pentamethylimdazolium (P) in a ratio of **2**/P = 9 was used as the OSDA. [2]**2**/P = 4, [3]**2**/P = 2.3.

Si/Ge	Si/Al	H_2O/TO_2	Temp. (°C)	Seeds	Time	Results

2	∞	5	175	None	6	STW + dense
9	∞	5	175	None	16	STW + U
∞	∞	5	175	None	23	BEA + dense
2	∞	<3	175	None	4	IWV
9	∞	<3	175	None	4	IWV
∞	∞	<3	175	None	20	Si-RTH layered
2	∞	4	175	None	4	IWV + STW
2	∞	5	175	None	4	IWV + STW
2	∞	7	175	None	4	IWV + STW
10	∞	4	175	None	4	IWV + CIT-7
10	∞	5	175	None	4	IWV
10	∞	7	175	None	4	IWV
2	∞	5	175	Si-STW	4	STW
10	∞	5	175	Si-STW	4	IWV + STW
2	∞	5	160	Si-STW	3	STW + U
∞	∞	4	175	None	13	Si-RTH layered
∞	∞	5	175	None	13	Si-RTH layered
∞	∞	7	175	None	36	Dense
10	∞	5	160	Si-STW	8	STW
∞	∞	5	160	Si-STW	11	Si-RTH layered
∞	∞	5	175	Si-STW	11	Si-RTH layered
10	∞	5	160	Si-STW	23	STW
15	∞	5	160	Si-STW	16	STW
20	∞	5	160	Si-STW	16	MTW
20	∞	5	160	Si-STW	16	MTW
10	∞	5	160	Si-STW	13	STW + IWV
15	∞	5	160	Si-STW	13	STW + IWV
20	∞	5	160	Si-STW	7	STW
20	∞	5	160	Si-STW	18	STW + IWV
20	∞	5	160	Si-STW	18	STW + IWV

30	∞	5	160	Si-STW	7	IWV
30	∞	5	160	Si-STW	7	IWV
50	∞	5	160	Si-STW	18	STW + IWV
50	∞	5	160	Si-STW	18	IWV
10	∞	4	160	Si-STW	20	STW
10	∞	7	160	Si-STW	5	IWV + STW
10	∞	7	160	Si-STW	5	IWV + STW
20	∞	4	160	Si-STW	20	STW
20	∞	7	160	Si-STW	5	IWV + STW
20	∞	10	160	Si-STW	5	IWV
30	∞	4	160	Si-STW	20	STW+amph
30	∞	7	160	Si-STW	12	IWV
30	∞	10	160	Si-STW	20	IWV
∞	∞	4	160	Si-STW	37	STW + layered[1]
∞	∞	4	160	Si-STW	37	STW[2]
∞	∞	4	160	Si-STW	20	STW[3]
∞	∞	2	160	None	14	MTW + STW
∞	∞	2	160	None	14	MTW + STW
∞	∞	3	160	None	14	MTW + STW
∞	∞	3	160	None	19	MTW + STW
4	∞	5	160	None	7	LTA
8	∞	5	160	None	7	LTA
20	∞	5	160	Si-STW	7	LTA + U
100	∞	5	160	Si-STW	30	A
20	∞	5	160	Si-STW	8	U
8	∞	4	160	Si-STW	10	U
10	∞	4	160	Si-STW	24	U
12	∞	4	160	Si-STW	10	U + A
14	∞	4	160	Si-STW	10	U + A
10	∞	4	160	Si-STW	13	IWV + LTA

2	∞	5	160	Si-STW	10	STW
2	∞	5	160	Si-STW	10	LTA + A
4	∞	5	160	Si-STW	10	LTA + U
4	∞	5	160	Si-STW	10	LTA + U
4	∞	5	160	Si-STW	13	STW + U
4	∞	5	160	Si-STW	13	STW + U
6	∞	5	160	Si-STW	13	STW + U
6	∞	5	160	Si-STW	13	STW + U
8	∞	5	160	Si-STW	29	LTA + U
8	∞	5	160	Si-STW	29	LTA + U
10	∞	5	160	Si-STW	29	LTA + U
10	∞	5	160	Si-STW	29	LTA + U
8	∞	5	160	Si-STW	11	LTA
8	∞	5	160	Si-STW	11	LTA
2	100	5	160	Si-STW	13	STW + LTA
2	100	5	160	Si-STW	13	STW
12	∞	5	160	Si-STW	11	LTA
12	∞	5	160	Si-STW	11	LTA

Table S2. Summary of STW syntheses using R-**2**. A = amorphous, U = unknown, synthesis time is reported in days.

Si/Ge	Si/Al	H_2O/TO_2	Temp. (°C)	Seeds	Time	Results
20	∞	4	160	Si-STW	16	STW
20	∞	4	160	Si-STW	16	RTH
20	∞	4	160	Si-STW	16	RTH + IWV + STW
20	∞	4	160	Si-STW	16	RTH
30	∞	4	160	Si-STW	16	RTH
2	100	4	160	Si-STW	10	STW
2	100	4	160	Si-STW	10	STW + LTA

2	100	4	160	Si-STW	10	STW + LTA + U
2	100	4	160	Si-STW	10	STW + LTA

Table S3. Summary of STW syntheses using S-**2**. A = amorphous, U = unknown, synthesis time is reported in days.

Si/Ge	Si/Al	H_2O/TO_2	Temp. (°C)	Seeds	Time	Results
20	∞	5	160	None	10	IWV+STW
20	∞	5	160	Si-STW	5	IWV+STW
5	∞	5	160	None	5	STW + tiny IWV
5	∞	5	175	Si-STW	5	IWV+STW
∞	∞	5	160	Si-STW	8	MTW + STW
∞	∞	5	160	None	8	MTW + STW
20	∞	4	160	Si-STW	13	STW
20	∞	4	160	Si-STW	13	STW
20	∞	4	160	Si-STW	25	A
20	∞	4	160	Si-STW	25	A
10	∞	4	160	Si-STW	24	LTA + U
10	∞	4	160	Si-STW	24	LTA + U
2	∞	5	160	Si-STW	12	STW + LTA
2	∞	5	160	Si-STW	12	STW + LTA
2	∞	5	160	Si-STW	12	STW
2	∞	5	160	None	12	STW + LTA
2	∞	5	160	None	12	LTA + U
2	100	5	160	Si-STW	13	STW
2	100	5	160	Si-STW	12	STW
2	100	5	160	Si-STW	13	STW + LTA
2	100	5	160	Si-STW	20	STW + LTA

Powder X-ray diffraction data (PXRD) data were collected on a Rigaku MiniFlex II with Cu Kα radiation.

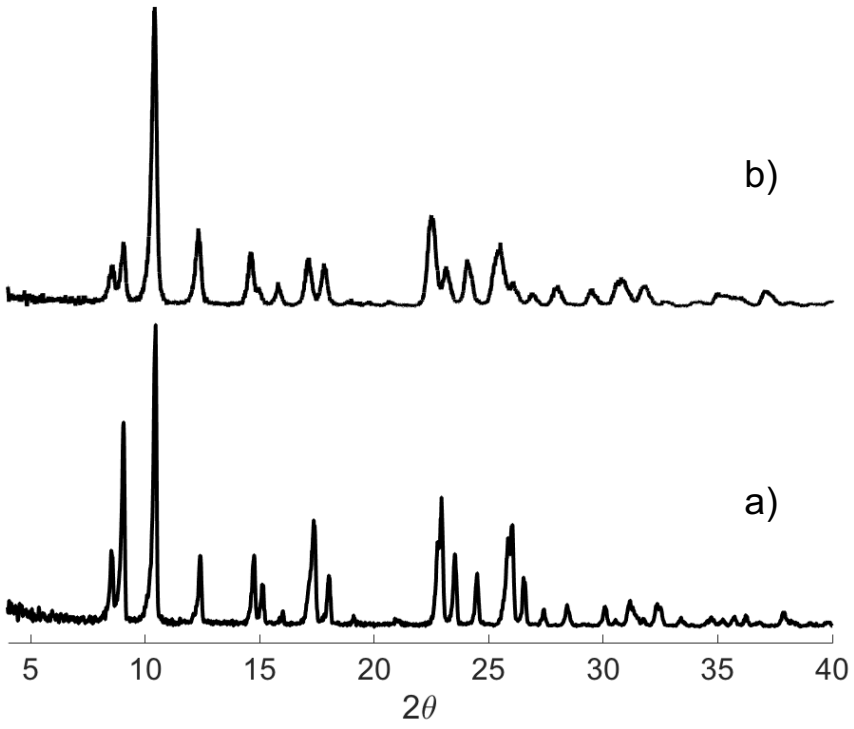

Fig. S3. Representative PXRD diffraction patterns for a) pure-silica racemic STW and b) germanosilicate enantrioenriched S-STW. The d-spacings in the enantioenriched sample are shifted as a consequence of the germanium content.

^{13}C, ^{19}F, ^{27}Al and ^{29}Si solid-state NMR were performed using a Bruker DSX-500 spectrometer (11.7 T) and a Bruker 4mm MAS probe. The spectral operating frequencies were 500.2 MHz, 125.721 MHz, 130.287 MHz and 99.325 MHz for ^{1}H, ^{13}C, ^{19}F, ^{27}Al and ^{29}Si nuclei, respectively. Spectra were referenced to external standards as follows: tetramethylsilane (TMS) for ^{1}H and ^{29}Si, $CFCl_3$ for ^{19}F, adamantane for ^{13}C as a secondary external standard relative to tetramethylsilane and 1.0 M $Al(NO_3)_3$ aqueous solution for ^{27}Al. Samples were spun at 14 kHz for ^{1}H and ^{27}Al MAS NMR and 8 kHz for ^{13}C and ^{29}Si MAS and CPMAS NMR experiments. ^{19}F MAS NMR were collected at both 13 and 15 kHz to assign spinning sidebands. For detection of ^{27}Al signal, a short 0.5μs - π/18 pulse was used before FID was recorded in order to make quantitative comparison among resonances.

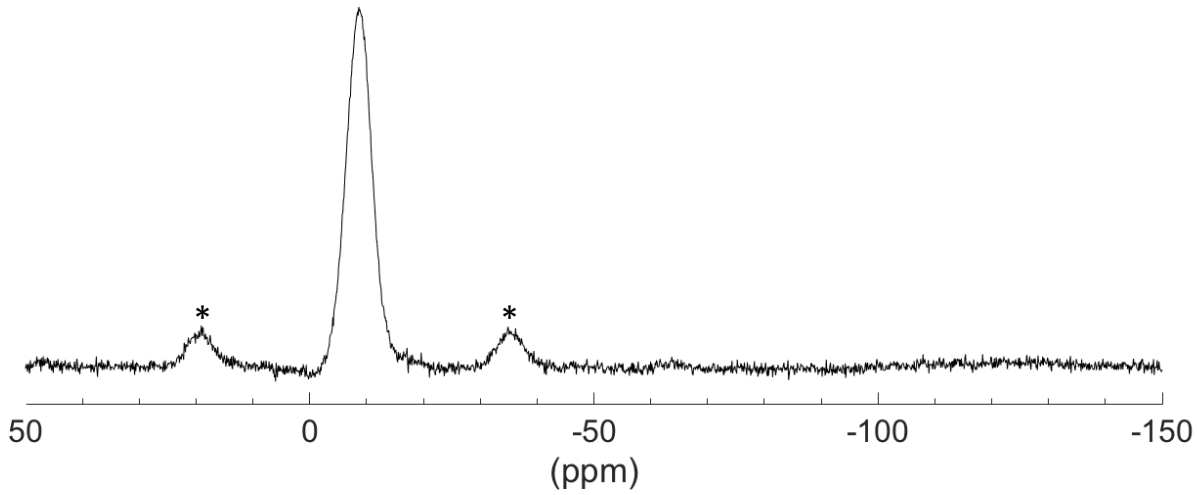

Fig. S4. ^{19}F NMR spectrum for an enantioenriched S-STW germanosilicate sample. Peaks labeled with a * correspond to spinning side bands.

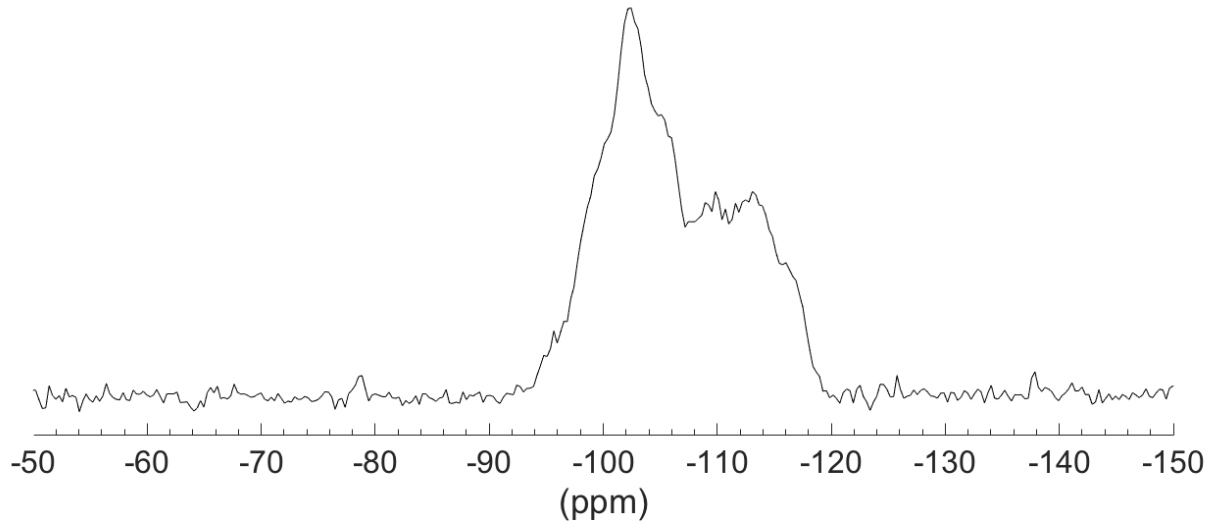

Fig. S5. ^{29}Si NMR spectrum for an enantioenriched S-STW germanosilicate sample.

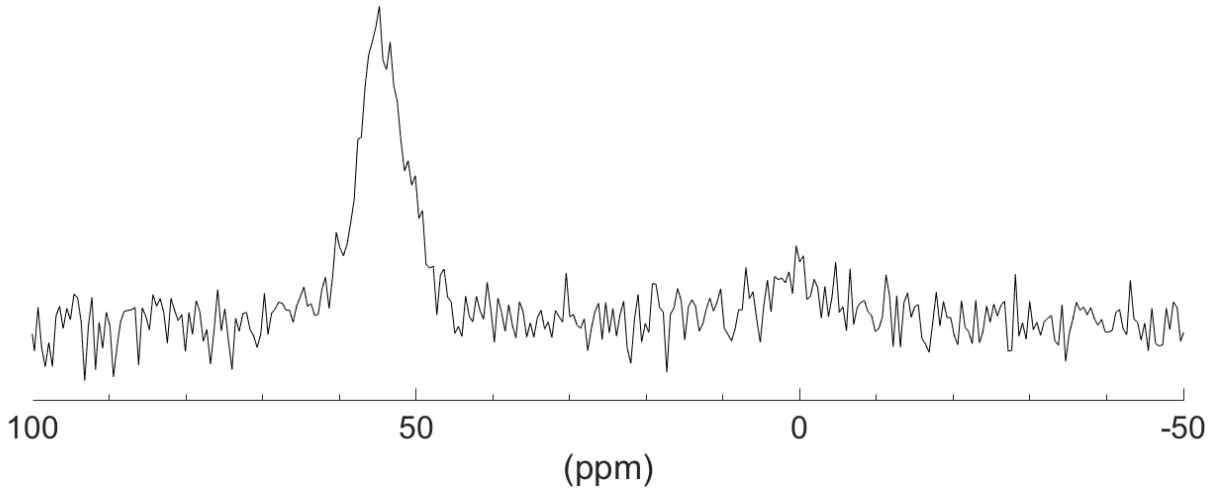

Fig. S6. ^{27}Al NMR spectrum for an enantioenriched S-STW aluminogermanosilicate sample.

Thermogravimetric analysis (TGA) measurements were performed on Perkin Elmer STA 6000. Samples (0.01-0.06 g) were placed in an alumina crucible and heated at 1 K/min in a flowing stream (0.667 cm^3/s) of air.

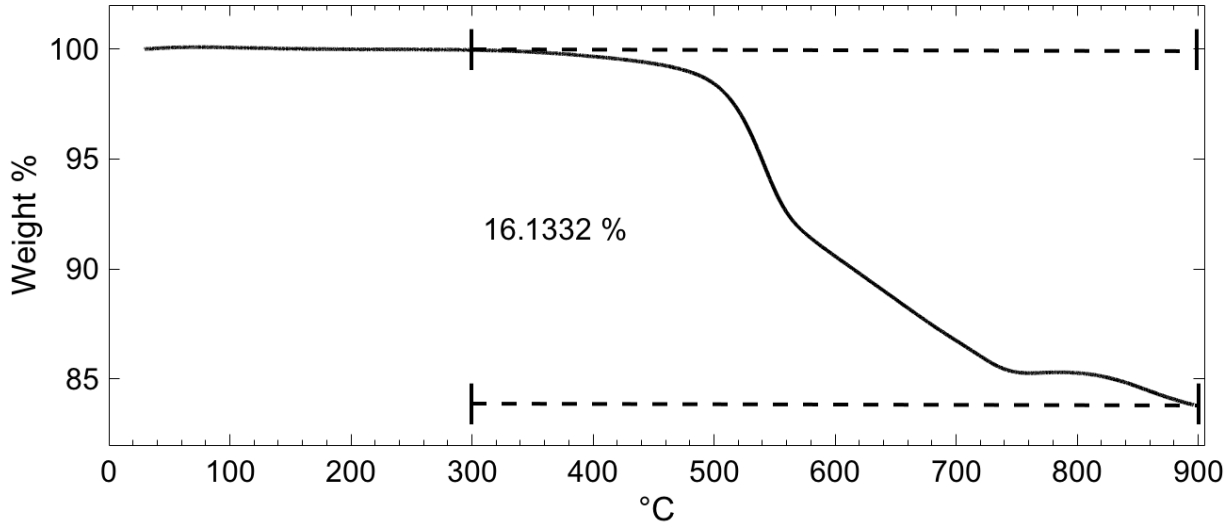

Fig. S7. A representative TGA profile for enantioenriched germanosilicate S-STW.

Scanning electron micrographs (SEM) were recorded on a Hitachi S-570 instrument. EDS spectra were acquired with an Oxford X-Max SDD X-ray Energy Dispersive Spectrometer system on a ZEISS 1550 VP FESEM, equipped with in-lens SE.

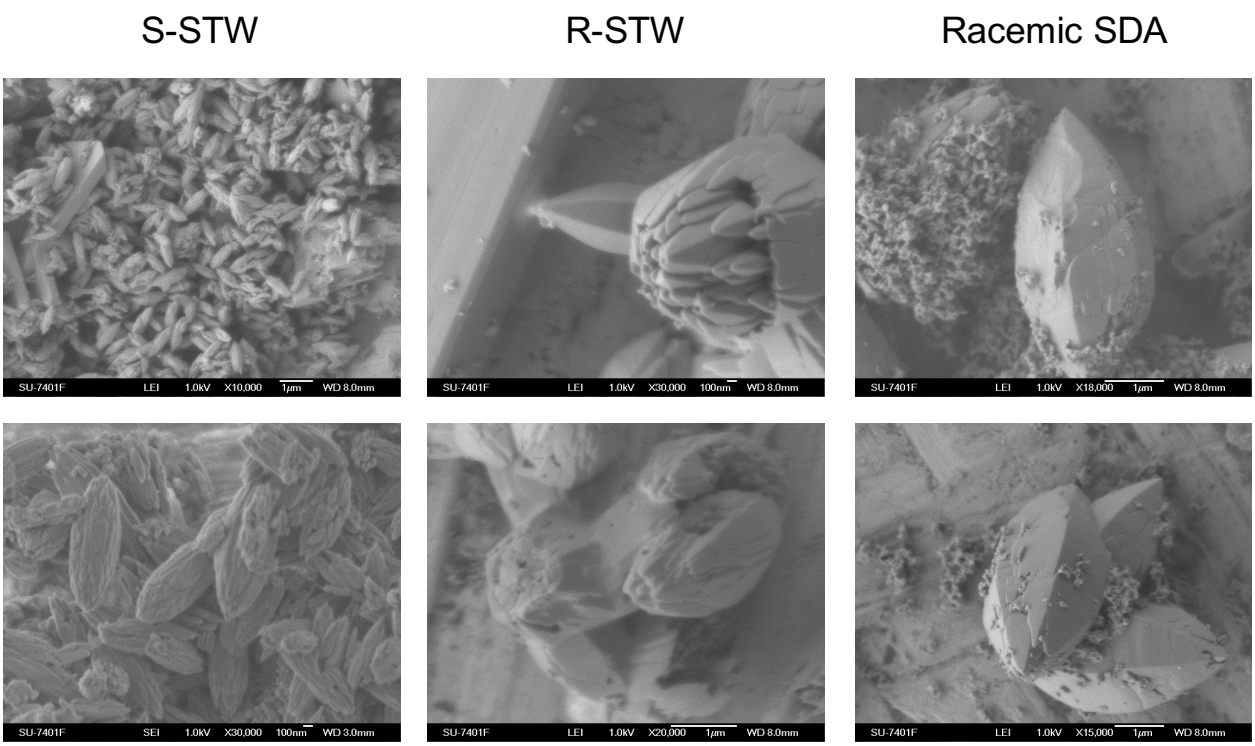

Fig. S8. Select SEM images for S-, R- and racemic STW.

EDS spectra were acquired with an Oxford X-Max SDD X-ray Energy Dispersive Spectrometer system on a ZEISS 1550 VP FESEM, equipped with in-lens SE.

Table S4. Representative energy-dispersive X-Ray spectroscopy results for products obtained using S-**2** in germanosilicate and aluminogermanosilicate synthesis gels.

Starting Gel	Si/Ge	Si/Al
Germanosilicate, Si/Ge = 2	0.806 ± 0.047	-
Aluminogermanosilicate, Si/Ge = 2; Si/Al = 100	0.861 ± 0.045	30.15 ± 11.96

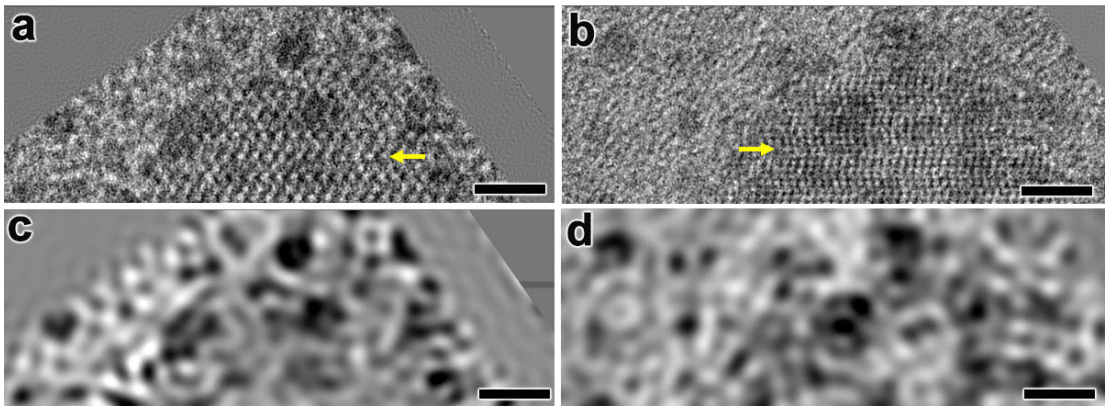

Fig S9. Comparison of two HRTEM images with gold nanoparticles as markers. **a,b,** A crystal was tilted from $[2\bar{1}\bar{1}0]$ (**a**) to $[1\bar{1}00]$ (**b**) and a shift-up was observed, which indicates a space group of $P6_522$. **c**,**d**, The processed images of (**a**) and (**b**) after Fourier filtering that only includes spatial frequencies within a particular range to enhance the contrasts of gold nanoparticles.

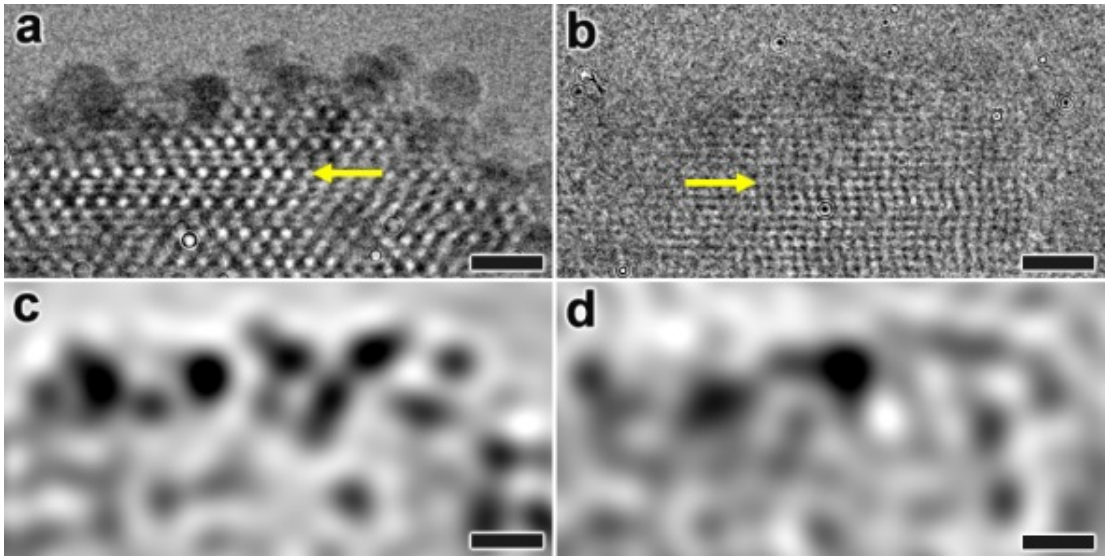

Fig. S10. Comparison of two HRTEM images with gold nanoparticles as markers. **a,b,** A crystal was tilted from $[2\bar{1}\bar{1}0]$ (**a**) to $[1\bar{1}00]$ (**b**) and a shift-down was observed, which indicates a space group of $P6_122$. **c**,**d**, The processed images of (**a**) and (**b**) after Fourier filtering that only includes spatial frequencies within a particular range to enhance the contrasts of gold nanoparticles.

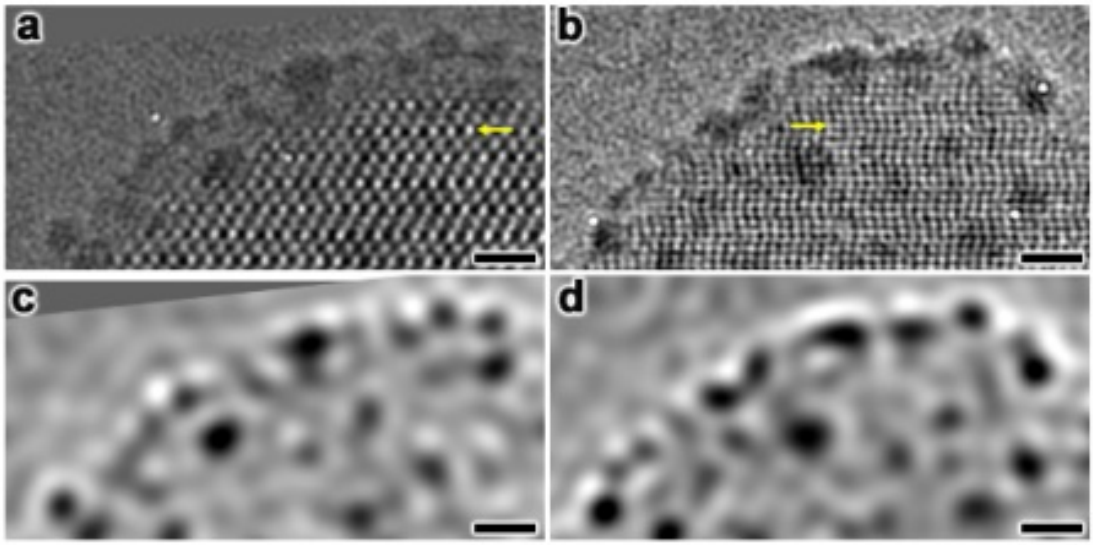

Fig. S11. Comparison of two HRTEM images with gold nanoparticles as markers. **a,b,** A crystal was tilted from $[2\bar{1}\bar{1}0]$ (**a**) to $[10\bar{1}0]$ (**b**) and a shift-up was observed, which indicates a space group of $P6_122$. **c**,**d**, The processed images of (**a**) and (**b**) after Fourier filtering that only includes spatial frequencies within a particular range to enhance the contrasts of gold nanoparticles.

4. Reaction and Analysis Procedures

After addition of 20 mg of Al-containing STW (Si/Al = 30 ± 10), 20 mmol of epoxide substrate, and 5 g of methanol (with pre-dissolved naphthalene as internal standard) were added to a 10 mL thick-walled glass reactor (VWR) containing a stir bar. The reactor was crimp-sealed and placed in a temperature-controlled oil bath at the desired reaction temperature. At predetermined times, aliquots of (~100 μL) were extracted and analyzed.

Quantitative GC/FID analysis was performed on an Agilent 7890B GC system equipped with a flame ionization detector and an Agilent Cyclosil-B column. Liquid ^{1}H and ^{13}C NMR spectra were recorded with a Varian INOVA 500 MHz spectrometer equipped with an auto-x pfg broad band probe. All liquid NMR analysis was performed in deuterated methanol.

5. Adsorption Procedures

Adsorption isotherms were collected on a Quantachrome Autosorb iQ with varying methods depending upon the adsorbate.

6. References

1. Pophale R, Daeyaert F, Deem MW (2013) Computational prediction of chemically synthesizable organic structure directing agents for zeolites. *J Mater Chem A* 1(23):6750–6760.
2. Schmidt JE, Deem MW, Davis ME (2014) Synthesis of a specified, silica molecular sieve by using computationally predicted organic structure-directing agents. *Angew Chemie - Int Ed* 53(32):8372–8374.
3. Overberger CG, Shimokawa Y (1971) Synthesis and Optical Properties of Asymmetric Polyamides Derived from Optically Active Dicarboxylic Acids and Spirodiamine. *Macromolecules* 4(6):718–725.
4. Cheng K, et al. (2011) Probes for Narcotic Receptor Mediated Phenomena. 41. Unusual Inverse μ-Agonists and Potent μ-Opioid Antagonists by Modification of the N-Substituent in Enantiomeric 5-(3-Hydroxyphenyl)morphans. *J Med Chem* 54(4):957–969.
5. Gottstein WJ (1969) US Patent 3,454,626.
6. Inouye Y, Sugita T, Walborsky HM (1964) Cyclopropanes—XVII: The absolute configurations of trans-1,2-cyclopropanedicarboxylic acid and trans-2-phenylcyclopropanecarboxylic acid. *Tetrahedron* 20(1961):1695–1699.
7. Taylor RJK, Campbell L, McAllister GD (2003) *Organic Syntheses* (John Wiley & Sons, Inc., Hoboken, NJ, USA) doi:10.1002/0471264229.os085.03.
8. de la Fuente V, et al. (2010) Phosphine ligands in the palladium-catalysed methoxycarbonylation of ethene: insights into the catalytic cycle through an HP NMR spectroscopic study. *Chemistry* 16(23):6919–32.
9. Pasquini C, Desvergnes-Breuil V, Jodry JJ, Dalla Cort A, Lacour J (2002) Chiral anion-mediated asymmetric induction onto chiral diquats. *Tetrahedron Lett* 43(3):423–426.
10. Lacour J, Vial L, Herse C (2002) Efficient NMR Enantiodifferentiation of Chiral Quats with BINPHAT Anion. *Org Lett* 4(8):1351–1354.
11. Lacour J, Londez a, Goujon-Ginglinger C, Buss V, Bernardinelli G (2000) Configurational ordering of cationic chiral dyes using a novel C(2)-symmetric hexacoordinated phosphate anion. *Org Lett* 2(26):4185–8.
12. Herse C, et al. (2003) A highly configurationally stable [4]heterohelicenium cation. *Angew Chemie - Int Ed* 42:3162–3166.
13. Rojas A, Camblor MA (2012) A pure silica chiral polymorph with helical pores. *Angew Chemie - Int Ed* 51(16):3854–3856.